Monte Carlo study of population and alignment relaxation by trapped line radiation

A. Hishikawa* and T. Fujimoto
Department of Engineering Science, Kyoto University, Kyoto 606-01, Japan

P. Erman
Physics Department I, Royal Institute of Technology, S-100 44 Stockholm, Sweden
(Received 11 October 1994)

Population and alignment relaxation for the Doppler broadening case in the infinite plane parallel geometry has been studied in the range of the optical thickness at the line center between 10^{-3} and 10^{2}. The obtained population and alignment relaxation rates are compared with analytical estimates. The validity of two approximations used in the estimates, i.e., the complete frequency redistribution of absorbed and successively emitted photons and the pure-parabolic distribution of excited atoms, is discussed. Also studied is the mixing of the population and the alignment, which is due to the spatial anisotropy of the geometry. This mixing leads to the *self-alignment* effect, which develops at a sufficiently late time after excitation. A separate simulation with the alignment effect *omitted* has revealed that, at a large optical thickness, the population relaxation rate agrees with the result with the alignment effect *included*. It is therefore concluded that the previous estimate on the influence of the self-alignment to the population relaxation rate is too large. The velocity distribution of the excited atoms in the direction perpendicular to the planes shows an effectively lower (higher) temperature at the center (boundary) than the base temperature ($\approx 5\%$) under the self-alignment condition.

PACS number(s): 32.90.+a

I. INTRODUCTION

Radiation trapping has been an important subject in many fields of science; in astrophysics, for instance, this phenomenon has long been treated within the framework of radiative transfer [1] and plays an important role in studying stellar atmospheres. Various laboratory gas-phase experiments such as atomic collision experiments [2] could be influenced by the reabsorption of resonance radiation. The radiation trapping effect is especially important in radiative lifetime measurements not only because it effectively reduces the radiative decay rate [3,4], but also because it relaxes the alignment originally created by spatially anisotropic excitation that causes temporal changes of the spatial intensity distribution and polarization of the emitted radiation [5–7]. The latter effect makes the decay of the observed emission intensity no longer equivalent to that of the population of the upper state and leads to errors in measured lifetimes. The alignment relaxation manifests itself also in a Hanle signal as a coherence narrowing effect [8].

The problem was first treated theoretically as a diffusion of excited atoms [9]. This treatment was based on the assumption of a definite mean free path for the resonance photon. Holstein [3,4] and Biberman [10] introduced a probabilistic treatment for the free path of photons and derived a Boltzmann type integro-differential equation

$$\frac{\partial n(\mathbf{r},t)}{\partial t} = -\gamma n(\mathbf{r},t) + \gamma \int n(\mathbf{r}',t) G(\mathbf{r}',\mathbf{r}) d\mathbf{r}' , \tag{1}$$

where $n(\mathbf{r},t)$ is the atomic density at position $\mathbf{r}$ at time t and $G(\mathbf{r}',\mathbf{r})d\mathbf{r}'$ is the probability that a photon emitted from volume $d\mathbf{r}'$ at $\mathbf{r}'$ is absorbed by an atom at $\mathbf{r}$. The quantity γ is the transition probability of the resonance transition. The following type of solution to Eq. (1) is first looked for:

$$n(\mathbf{r},t) = n(\mathbf{r}) \exp(-\beta t) , \tag{2}$$

which transforms Eq. (1) into

$$\left[1 - \frac{\beta}{\gamma}\right] n(\mathbf{r}) = \int n(\mathbf{r}') G(\mathbf{r}',\mathbf{r}) d\mathbf{r}' . \tag{3}$$

The homogeneous integral equation (3) yields a set of positive eigenvalues $\beta^{(i)}$ and solutions $n^{(i)}(\mathbf{r})$. The general solution to Eq. (1) is therefore expressed as

$$n(\mathbf{r},t) = \sum_i c^{(i)} n^{(i)}(\mathbf{r}) \exp(-\beta^{(i)} t) , \tag{4}$$

where $c^{(i)}$ are coefficients depending on the initial conditions. After a sufficiently long time, only the component of the smallest $\beta^{(i)}$ in Eq. (4), or $\beta^{(0)}$, survives, leading to $n(\mathbf{r},t) \approx n^{(0)}(\mathbf{r}) \exp(-\beta^{(0)} t)$. This last surviving component is called *the fundamental decay mode* [3], which is independent of the initial distributions of excited atoms and their velocity. For various geometries and line profiles, Holstein [3,4] solved Eq. (3) by Ritz's variational

*Present address: Department of Pure and Applied Sciences, College of Arts and Sciences, The University of Tokyo, 3-8-1 Komaba, Meguro-ku, Tokyo 153, Japan.

method under optically thick conditions. Three major approximations were adopted for the purpose of simplifying the calculation: (i) the alignment of excited atoms is ignored, (ii) spatial distribution function of the excited atoms is pure parabolic, that is, the excited atom density tends to zero at the edges of the cell, and (iii) the frequency redistribution between the absorbed and the emitted photons is complete [complete frequency redistribution (CRD)], i.e., the frequency profile of emission from individual atoms $P(\nu)$ is assumed to be the same as that of absorption $k(\nu)$, when viewed in a spatially fixed frame. For the Doppler-broadening case, this approximation is fully justified in the infinite cell geometry, since the radiation field density is uniform. The absorption coefficient for the Doppler-broadening case is given as

$$k(\nu)=k_0\exp\left[-\frac{(1-\nu/\nu_0)^2}{(v_0/c)^2}\right], \tag{5}$$

$$k_0=\frac{1}{8\pi^{3/2}}\frac{g_1}{g_0}\frac{c^3\gamma N}{v_0\nu_0^3}, \tag{6}$$

$$v_0=\left[\frac{2k_BT}{m}\right]^{1/2}. \tag{7}$$

Here N is the atomic number density, ν_0 is the central frequency of the resonance line, g_0 and g_1 are the statistical weights of the ground and the excited state, respectively, k_B is the Boltzmann constant, T is the temperature, and m is the mass of the atom. The relaxation rate $\beta^{(0)}$ at the high optical thickness limit for an infinite plane parallel geometry with the half spacing length L is approximately given by

$$\beta^{(0)}=\gamma\frac{0.9375}{k_0L(\pi\ln k_0L)^{1/2}}. \tag{8}$$

The state of an ensemble of atoms is fully described in terms of a density matrix, in which the diagonal elements represent the population of magnetic sublevels and the off-diagonal elements represent coherence between these sublevels. Assuming that all atoms have the same speed, Barrat [11] developed a theory with the density-matrix formalism that describes the time evolution of the population and the alignment in excited states. Later, D'Yakonov and Perel' [12] extended the theory also to the orientation with a more realistic velocity distribution, that is, a Maxwell distribution.

According to D'Yakonov and Perel' [12], relaxation of various quantities in the excited state by the trapped radiation is expressed in terms of the state multipoles $\langle T(J)^\dagger_{KQ}\rangle(\mathbf{r},\mathbf{p},t)$ [13] as

$$\frac{d}{dt}\langle T(J)^\dagger_{KQ}\rangle=-\gamma\langle T(J)^\dagger_{KQ}\rangle+\gamma\int\int d\mathbf{r}'d\mathbf{p}'\sum_{K',Q'}S^{K'Q'}_{KQ}(\mathbf{r}-\mathbf{r}',\mathbf{p},\mathbf{p})\times\langle T(J)^\dagger_{K'Q'}\rangle. \tag{9}$$

As seen from this equation, state multipoles are coupled each other by the matrix S. The state multipoles $\langle T(J)^\dagger_{00}\rangle$, $\langle T(J)^\dagger_{10}\rangle$, and $\langle T(J)^\dagger_{20}\rangle$ have clear physical meanings [13]: these quantities are proportional to the population, the orientation, and the alignment, respectively, of the excited state. Therefore, Eq. (9) is a generalization of Eq. (1). Under the CRD assumption, D'Yakonov and Perel' [12] have derived a solution for the cell without boundaries. The state multipoles become independent of $\mathbf{r}$ so that Eq. (9) reduces to a simple form

$$\frac{d}{dt}\langle T(J)^\dagger_{KQ}\rangle=-\gamma^\infty_K\langle T(J)^\dagger_{KQ}\rangle, \tag{10}$$

where

$$\gamma^\infty_K=\gamma(1-\alpha_K),\quad K=0,1,2 \tag{11}$$

$$\alpha_K=\tfrac{3}{10}(2j_1+1)[6+(-1)^K]\begin{Bmatrix}1 & 1 & K\\ j_1 & j_1 & j_0\end{Bmatrix}^2, \tag{12}$$

where j_0 and j_1 are the angular momenta of the lower and the upper states, respectively. The value of α_K is tabulated, for instance, in Ref. [8]. As is seen in Eq. (11), the state multipoles of each rank relax independently. In other words, there is no mixing of the state multipoles of different ranks.

For an infinite plane parallel geometry, the symmetric geometry simplifies Eq. (9) to a large extent

$$\frac{d}{dt}\langle T(J)^\dagger_{00}\rangle=-\gamma\langle T(J)^\dagger_{00}\rangle+\gamma\int\int d\mathbf{r}'d\mathbf{p}'S^{00}_{00}(\mathbf{r}-\mathbf{r}',\mathbf{p},\mathbf{p}')\langle T(J)^\dagger_{00}\rangle+\gamma\int\int d\mathbf{r}'d\mathbf{p}'S^{20}_{00}(\mathbf{r}-\mathbf{r}',\mathbf{p},\mathbf{p}')\langle T(J)^\dagger_{20}\rangle, \tag{13}$$

$$\frac{d}{dt}\langle T(J)^\dagger_{20}\rangle=-\gamma\langle T(J)^\dagger_{20}\rangle+\gamma\int\int d\mathbf{r}'d\mathbf{p}'S^{20}_{20}(\mathbf{r}-\mathbf{r}',\mathbf{p},\mathbf{p}')\langle T(J)^\dagger_{20}\rangle+\gamma\int\int d\mathbf{r}'d\mathbf{p}'S^{00}_{20}(\mathbf{r}-\mathbf{r}',\mathbf{p},\mathbf{p}')\langle T(J)^\dagger_{00}\rangle, \tag{14}$$

where the orientation $\langle T(J)^\dagger_{10}\rangle$ has been assumed to be absent according to the initial condition. At optically thick conditions, the contribution from the off-diagonal term in Eqs. (13) and (14) becomes small because the integral operator approaches zero in the limit of high optical thickness [14]

$$\int d\mathbf{r}'S^{K'0}_{K0}(\mathbf{r}-\mathbf{r}',\mathbf{p},\mathbf{p})\to(1-\alpha_K)\delta_{KK'}. \tag{15}$$

When the optical thickness is large enough, this applies to most positions $\mathbf{r}$ in the cell.

By neglecting the off-diagonal term in the equations, D'Yakonov and Perel' [12] obtained qualitative estimates of the relaxation rates of the population (γ_0) and the alignment (γ_2) in an infinite plane parallel geometry. Again assumed, as in the case of Eq. (10), are the CRD approximation, the Doppler broadening, and a pure-parabolic population distribution function. The relaxation rates are expressed in terms of parameter x_K, which depends on the optical thickness and the cell geometry

$$\gamma_K=\gamma(1-\alpha_K x_K),\quad K=0,1,2,\ . \tag{16}$$

For the infinite plane parallel geometry, x_2 is obtained by the variational method [12]

$$x_2=1-\frac{75/64}{k_0L(\pi\ln k_0L)^{1/2}}\quad (k_0L\gg 1)\ . \tag{17}$$

From Eq. (8), the x_0 in the fundamental decay mode is derived as

$$x_0=1-\frac{0.9375}{k_0L(\pi\ln k_0L)^{1/2}}\ . \tag{18}$$

The quantity $(1-x_0)$ is called the escape factor for the fundamental decay mode of the population [3].

After a sufficiently long time, $\langle T(J)^\dagger_{20}\rangle$ is much smaller than $\langle T(J)^\dagger_{00}\rangle$ under optically thick conditions so that the contribution from $\langle T(J)^\dagger_{20}\rangle$ to $\langle T(J)^\dagger_{20}\rangle$ itself [the diagonal term in Eq. (14)] becomes insignificant. Accordingly the relaxation rate of $\langle T(J)^\dagger_{20}\rangle$ becomes small compared to γ_2 and therefore the left-hand side of Eq. (14) is negligible. Thus it follows from Eq. (14) that

$$\langle T(J)^\dagger_{20}\rangle=\int\int d\mathbf{r}'d\mathbf{p}'S^{00}_{20}(\mathbf{r}-\mathbf{r}',\mathbf{p},\mathbf{p}')\langle T(J)^\dagger_{00}\rangle\ . \tag{19}$$

The equation shows that at a sufficiently late time the alignment relaxes at the same rate as the population. This situation is nothing but the *self-alignment* [14]. Although the self-alignment effect has been observed in discharge plasmas [15], a quantitative interpretation of the self-alignment due to the radiation trapping has not been established yet. Using Eq. (19), Perel' and Rogova [14] also estimated the influence of the mixing of alignment into population, expressed by the *off-diagonal* term of Eq. (13). The equation is solved by treating the off-diagonal term as a perturbation, leading to a decrease in the population relaxation rate by

$$\frac{\Delta\gamma_0}{\gamma_0}\approx\frac{1}{\ln k_0L}\ . \tag{20}$$

It was suggested that, when the self-alignment is destroyed by a weak magnetic field, the effective lifetime would decrease by this amount [14]. This assertion, however, appears rather puzzling because many experiments performed so far seem to suggest that Eq. (8), or a corresponding approximation for a cylindrical geometry, describes the observation rather well.

Unlike the analytical methods reviewed above, the Monte Carlo method can provide solutions to the fundamental equation, Eq. (9) or Eqs. (13) and (14), without any approximations. The relaxation rates γ_0 and γ_2 can be obtained by this method. The present work focuses especially on the mixing of different ranks of the state multipoles, the population $\langle T(J)^\dagger_{00}\rangle$, and the alignment $\langle T(J)^\dagger_{20}\rangle$ and on the validity of the approximations used in the analytical solutions Eqs. (17) and (18) such as CRD and the spatial distribution of the population.

II. MONTE CARLO METHOD

The Monte Carlo method has been employed for the radiative transfer problem by many researchers especially in astrophysics (see, for instance, Ref. [16]). In this method, any relevant quantities, say, the emission direction of a photon, its frequency, and free path, are determined by random numbers satisfying the individual probability density functions. In the present study an excited atom is described by an oscillating electric dipole that is equivalent to the pair of the angular momentum quantum numbers $j_0=0$ and $j_1=1$. The cell geometry is assumed to be infinite parallel planes with the separation $2L$ with a quantization axis (z axis) perpendicular to the planes. A Doppler-broadening line profile and a two-level atom are assumed.

The position of an originally excited atom in a cell is determined according to the distribution function [3]

$$P(\zeta)=a_0n_0(\zeta)+a_1n_1(\zeta)\ ,$$
$$n_0=\tfrac{1}{2},\quad n_1=\tfrac{3}{4}(1-\zeta^2),\quad \zeta=z/L\ . \tag{21}$$

The atom is given a velocity chosen from the Maxwell distribution. The original alignment direction is set parallel to the quantization axis. The emission from this atom occurs after $\Delta t=-(1/\gamma)\ln u$, where γ is the transition probability of the resonance line and u is a random number distributed between 0 and 1. The emission is characterized by the free path ρ and the polar and azimuthal angles θ and φ with respect to the dipole (alignment) direction. These angles are determined by using different random numbers as [17]

$$\theta=\cos^{-1}[2\cos\{\tfrac{1}{3}\cos^{-1}(2u-1)+\pi/3\}]\ , \tag{22}$$

$$\varphi=2\pi u\ , \tag{23}$$

which produce the angular distribution of the dipole emission. Then the velocity component to the photon direction, or the frequency ν of the emission, is calculated. Assuming a negligible natural linewidth, the free path ρ of the emitted photon is represented as

$$\rho=-\frac{1}{k(\nu)}\ln u\ . \tag{24}$$

From these parameters, the position of the newly excited atom and its alignment direction are calculated. The polarization direction of the absorbed photon at the newly excited atom lies in the plane spanned by the direction of the original alignment and the photon propagation direction. The resonance scattering in the present case ($j_0=0$, $\Delta j=j_1-j_0=1$) can be treated identically to Rayleigh scattering [18]. Therefore, the direction of the induced alignment is the same as that of the polarization of the photon. According to this calculated alignment direction, one of the components (in x, y, or z direction) having a unit amplitude is chosen as a new alignment direction of the newly excited atom. The velocity component of the excited atom in the propagation direction of the absorbed photon is calculated from the frequency $v_\rho=c(\nu-\nu_0)/\nu_0$. The perpendicular component v_n and its angle ϕ around the photon propagation direction are determined again by random numbers

$$v_n^2=-v_0^2\ln u\ , \tag{25}$$

$$\phi=2\pi u\ . \tag{26}$$

The procedure is repeated until the photon escapes from the cell and is then restarted from another originally excited atom. Finally, all excited atoms existing in a cell at time t after the start are counted separately according to their alignment direction. The number of the excited atoms at time t may be referred to as $n_x(t), n_y(t), n_z(t)$, from which the population $n_0(t)$ and the alignment $n_2(t)$ are calculated as [13]

$$n_0(t)=n_x(t)+n_y(t)+n_z(t) , \tag{27}$$

$$n_2(t)=n_z(t)-n_0(t)/3 . \tag{28}$$

The half spacing (L) of the planes is set to 2.5×10^{-2} m. A resonance state of helium, the $3\,^1P$ state ($\gamma=5.66\times10^8\ s^{-1}$), is used as a model in the simulation. The branching transitions ($3\,^1P-3\,^1S, 2\,^1S$) are neglected for simplicity. The temperature is set equal to 15 °C (288.15 K). The uniform random numbers u are produced with a special care to ensure its randomness and uniformity. We use 20 different sets of random numbers u and summed the results to eliminate systematic errors. The total number of the initially excited atoms is between 10^6-10^7, requiring typically 1 h of CPU time on a FACOM M-1800 computer in the case of $k_0L=13.6$.

III. RESULTS AND DISCUSSION

A. Mixing of population and alignment

A typical example of the results is shown in Fig. 1(a), which plots the population and the alignment integrated over both the volume and the momentum at each time. The abscissa is the time after the start in units of the natural lifetime $\tau=1/\gamma$. The optical thickness at the line center (k_0L) is taken to be 13.6. The profile of the population distribution at a sufficiently late time is plotted in Fig. 2(a), which shows good agreement with the initial population distribution ($a_0/a_1=0.266$), represented by the solid curve. The population distribution is monitored also during the relaxation to make sure that the spatial profile is the same during the course of time. This ensures that the relaxation is essentially in the fundamental decay mode with the negligible amount of higher modes. The ratio a_0/a_1 decreases as the optical thickness increases; for instance, $a_0/a_1=0.219$ at $k_0L=45.2$. A similar tendency has been observed for the infinite cylinder geometry [19] by the propagator function method [20].

As is seen in Fig. 1(a), the alignment exhibits a double-exponential decay curve. The slower component of the alignment has the same relaxation rate as that of the population. This is more clearly presented in Fig. 1(b), in which the *normalized alignment* $n_2(t)/n_0(t)$ is plotted as a function of time. The slower component is attributed to the mixing of the population $\langle T(J)^{\dagger}_{00}\rangle$ to the alignment $\langle T(J)^{\dagger}_{20}\rangle$, or the *self-alignment effect* [see Eq. (19)]. The spatial distribution of the normalized alignment under this condition is plotted in Fig. 2(b); the self-alignment is almost constant in the inner region of the cell, while at the edge, where the optical thickness is approximately equal to 1, it turns into negative values. This

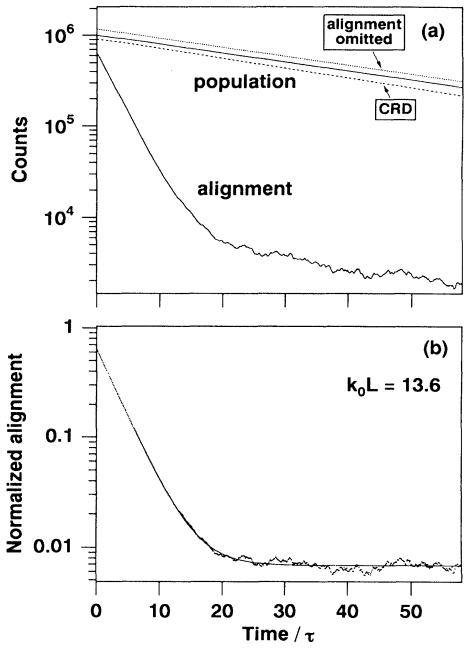

FIG. 1. (a) Typical example of the decay curves of the population and the alignment (solid curve). The optical thickness at the line center (k_0L) is 13.6. The simulation results with the alignment effect omitted is also plotted (dotted curve). Note that the population relaxation in this case is described by a single exponential curve. It is also shown that the CRD approximation gives substantially larger population relaxation rates (dashed curve). (b) Normalized alignment $n_2(t)/n_0(t)$ as a function of time. The simulation data are taken from (a). Note that the $n_2(t)/n_0(t)$ becomes constant after a sufficiently long time. Also shown is the result of the fitting from which the alignment relaxation rate γ_2 is obtained.

means that the alignment direction is perpendicular to the plane in the inner region, which implies that the excited atoms are created more by radiation propagating parallel to the plane than radiation perpendicular to the plane. On the contrary, atoms near the boundaries are excited more by radiation propagating perpendicularly to the plane. This picture is consistent with the population distribution of the excited atoms [Fig. 2(a)] showing that the atoms are concentrated near the central region. Perel' and Rogova [14] obtained the spatial distribution of the alignment by assuming a pure parabolic distribution ($a_0=0$) for the population. The self-alignment calculated from their results is also drawn in Fig. 2(b) for comparison. The value at $\zeta=0$ in their approximation is given as [14]

$$\frac{n_2(\zeta=0)}{n_0(\zeta=0)}=\frac{1}{1.2k_0L\,(2\pi\ln k_0L)^{1/2}} , \tag{29}$$

which is 1.62×10^{-2} in Fig. 2(b). Their results show that the normalized alignment changes its sign at a smaller ζ value than the present Monte Carlo results. This behavior is understood by the pure parabolic population distribution used in the estimate; this distribution suggests that there is no radiation parallel to the plane at the boundary.

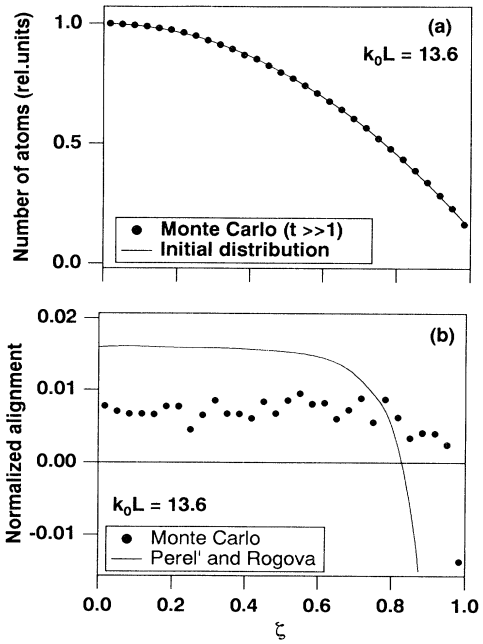

FIG. 2 (a) Spatial distribution of the population at a sufficiently late time with $k_0L=13.6$. The initial distribution ($a_0/a_1=0.266$) is also shown for comparison. (b) Spatial distribution of the self-alignment. The analytical result by Perel' and Rogova [14] is also shown.

From Eq. (19), the amount of the self-alignment may be defined as

$$\frac{\langle T(J)^{\dagger}_{20}\rangle}{\langle T(J)^{\dagger}_{00}\rangle}=\frac{\int\int d\mathbf{r}'d\mathbf{p}'S^{00}_{20}(\mathbf{r}-\mathbf{r}',\mathbf{p},\mathbf{p}')\langle T(J)^{\dagger}_{00}\rangle}{\langle T(J)^{\dagger}_{00}\rangle}\ . \tag{30}$$

As seen on the right-hand side of this equation, the self-alignment gives an effective value of the off-diagonal mixing matrix component. The normalized alignment at $t\gg\tau$ in a plot such as Fig. 1(b) gives the self-alignment averaged over volume and momentum, which is shown in Fig. 3 for several values of k_0L. The figure shows that the self-alignment decreases as the optical thickness increases, consistent with Eq. (15). The fact that the self-alignment is constant in the central region where the most excited atoms are concentrated allows us to use Eq. (29) as an estimate of the integrated self-alignment. As seen in the figure, this estimate is systematically larger by a factor of 2.5.

For the purpose of investigating the influence of the self-alignment on the population relaxation rate as discussed in Ref. [14], a separate simulation is done in which the alignment effect is omitted: the emission distribution from an atom is set isotropic by replacing the emission distribution function Eq. (22) with $\theta=\cos^{-1}(1-2u)$. The results (dotted line in Fig. 1) show that after a sufficiently late time the population relaxation rate agrees with the one obtained with the alignment effect *included* [Fig. 1(a)] within 1% at $k_0L=13.6$. This agreement appears quite reasonable when we note the small self-alignment (<0.01)

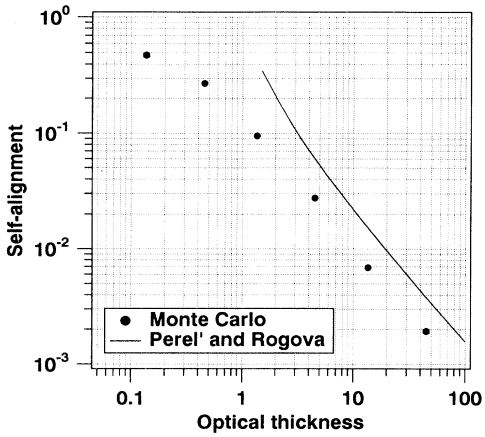

FIG. 3. Self-alignment against k_0L. Values at $k_0L<0.1$ are not obtained because of the poor statistics. The solid line represents Eq. (29) from Perel' and Rogova [14].

at $k_0L>10$ in Fig. 3, because the mixing of the alignment to the population would be insignificant in case of $\langle T(J)^{\dagger}_{00}\rangle\gg\langle T(J)^{\dagger}_{20}\rangle$. On the other hand, Eq. (20) gives an about 40% decrease due to the rank mixing effect. The reason for the large discrepancy is not fully identified yet, but the overestimate of the self-alignment shown in Fig. 3 caused by the nonrealistic distribution of excited atoms would be responsible, at least partly, for this difference.

The solid line in Fig. 1(a) shows a trace of the mixing effect in the population relaxation at $t<3\tau\approx1/(\gamma_0-\gamma_2)$, where the relaxation rate is found to be about 8% lower than the rate at $t>1/(\gamma_0-\gamma_2)$. This is because the alignment $\langle T(J)^{\dagger}_{20}\rangle$ is so large in the beginning of the relaxation that the contribution from the mixing term becomes substantial. The lengthening of the effective lifetime in this time domain by this mixing is understood from Eq. (13). This slow relaxation is not observed in the separate simulation with the alignment effect *omitted* (dotted line).

B. Population and alignment relaxation rates

The population relaxation rate γ_0 is estimated from the straight-line part of the relaxation curves at $t>1/(\gamma_0-\gamma_2)$ where the mixing effect is minimal. The faster component in the alignment relaxation in Fig. 1(a) corresponds to the alignment relaxation rate γ_2. We derive γ_2 from the decay curve in Fig. 1(b) by fitting it to a single exponential curve with a constant background. The fitting is done in the same time region as for γ_0. The population relaxation rates obtained at $k_0L>1$ are regarded as that for the fundamental decay mode since the rate and the population distribution stay constant during the relaxation. The situation is less clear for alignment since, because of the self-alignment effect, the alignment distribution profile is not fully examined to have the same profile in the course of time. However, an excellent fit to a single-exponential curve, such as the one shown in Fig. 1(b), may imply the presence of the fundamental decay

mode for the alignment, although no clear theoretical demonstration has been presented yet [12]. The accuracy of the obtained relaxation rates is estimated to be about 0.1% at high optical thicknesses.

Obtained relaxation rates γ_0 and γ_2 for the present geometry are expressed in terms of parameters x_0 and x_2 through Eq. (16). In Fig. 4, $(1-x_K)$ are plotted as a function of k_0L. For low to intermediate optical thickness ($k_0L<1$), obtained relaxation curves should be treated with caution since the large mixing between the population and the alignment (Fig. 3) makes it difficult to separate these two components. Therefore, only effective rates both for the population and the alignment relaxation are plotted in Fig. 4 for $k_0L<0.1$. For comparison, also shown are the analytical estimates by Holstein for population [Eq. (18)] and by D'Yakonov and Perel' for alignment [Eq. (17)]. As seen in the figure, the estimate by Holstein shows good agreement with the present results at high optical thickness with a discrepancy of 8.9% and 2.1% at $k_0L=13.6$ and 45.2, respectively. Holstein estimated the error in Eq. (8) due to the CRD approximation to be less than 20% at $k_0L=100$ [3].

Figure 5(a) shows the radiation field in the direction perpendicular to the planes at the center and at the boundaries of the cell, respectively. The solid angle of detection is 0.79 sr. The distribution of velocity component in the z direction of excited atoms is shown in Fig. 5(b). The profiles are narrower at the center and wider at the boundary than the Maxwell distribution at the base temperature, respectively. This is explained from the radiation field density [Fig. 5(a)]. At the center of the geometry, the atoms experience a stronger radiation field at the line center than at the line wings, while at the boundaries of the geometry the radiation field is stronger

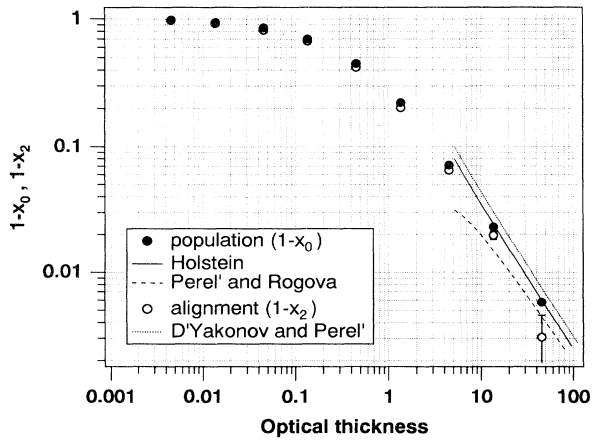

FIG. 4. Relaxation parameters of the population $(1-x_0)$ and the alignment $(1-x_2)$ for the infinite plane parallel geometry plotted as a function of k_0L. The quantity $(1-x_0)$ at $k_0L>1$ is considered to be values in the fundamental decay mode. Analytical estimates by Holstein [3] [Eq. (18)], D'Yakonov and Perel' [12] [Eq. (17)], and Perel' and Rogova [14] [Eq. (20)] are also shown for comparison. Only effective values are plotted for $k_0L<0.1$ because of the large mixing between the population and the alignment.

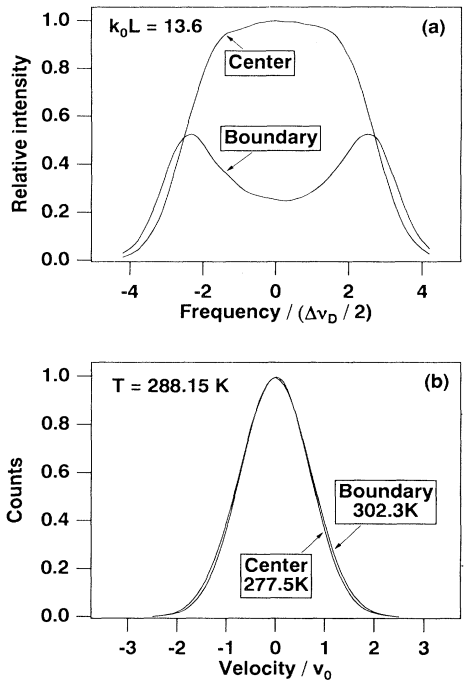

FIG. 5. (a) Radiation field intensity in the direction perpendicular to the plane as a function of the frequency. The solid angle of detection is 0.79 sr. The self-reversal effect is observed at the boundary. (b) Velocity distribution in the perpendicular direction to the plane after a sufficiently long time. The effective temperature is also presented, which is obtained by the Gaussian fit to the distributions.

at the line wings than at the line center *(self-reversal effect)*. Therefore the velocity distribution at the center (boundary) is enhanced at the center (wings) of the profile. The difference between the two profiles in Fig. 5(b) is not as pronounced as expected from the radiation field shown in Fig. 5(a) since excited atoms are also created by the radiation propagating parallel to the plane and these atoms have the Maxwell velocity distribution of the base temperature in the direction perpendicular to the plane. The influence of velocity relaxation from the initial to the distribution shown in Fig. 5(b) on the relaxation rates γ_0, γ_2 is considered to be negligible because the velocity relaxation is estimated to be so fast (the rate is of the order of γ) [21] that the component has relaxed out at the time interval when γ_0 and γ_2 are estimated.

In Fig. 1(a) also plotted is a decay curve obtained with the CRD approximation with *the alignment effect included* (dashed line). At this optical thickness, the population relaxation rate increases significantly (9.9%). The increase in the population relaxation rate is found to be smaller (7.8%) at $k_0L=45.2$. This increase corresponds to the increase of the filled circle in Fig. 4. Thus the result of the CRD simulation is larger than Eq. (18), or the solid curve in Fig. 4, by 5% at $k_0L=45.2$. When the more realistic distribution of excited atoms as expressed in Eq. (21) are adopted in deriving Eq. (8), the population relaxation rate will be *reduced* by an amount [3]

$$\frac{\Delta\gamma_0}{\gamma_0} = -\frac{\frac{1}{16}}{\ln 2k_0L - \frac{5}{4}}, \tag{31}$$

which is about 2% at $k_0L=45.2$, leading to even a larger difference (7%) in $(1-x_0)$ from the simulation result. In Fig. 4 also plotted is the quantity $(1-x_0)$ obtained from γ_0 with the correction proposed in Ref. [14], Eq. (20), included. It is clearly shown that the influence of the rank mixing effect is overestimated in Ref. [14], as discussed in Sec. III A.

Figure 4 clearly shows that $(1-x_2)$ is systematically smaller than $(1-x_0)$, in contrast to the analytical estimate [12]. A separate simulation with the CRD approximation at $k_0L=45.2$ yields $(1-x_2)=5\times10^{-3}$ and reduces the large discrepancy between the present result and the estimate. The residual discrepancy may be attributed to the spatial distribution assumed in deriving Eq. (17), since the radiation field at the center of the cell is expected to become more isotropic when the distribution Eq. (21) is assumed, leading to a faster relaxation of the normalized alignment. If we compare the results by the simulation and the analytical method in terms of γ_2 rather than $(1-x_2)$ as in Fig. 4, the difference is less pronounced because of a small α_2 value in Eq. (16). For instance, the difference in γ_2 corresponding to the open circle and the dotted curve in Fig. 4 is only 1% at $k_0L=45.2$.

A time-resolved measurement of γ_K $(K=0,1,2)$ have been reported [22] for the He $3\,^1P$ state by the crossed electron-atom beam method. A comparison with the present results is, unfortunately, impractical, since the estimate of the atomic density in an effusive beam is difficult. Instead, the authors [22] suggested the use of the relaxation rate, or the relaxation parameter x, as a measure of the effective atomic density in the collision region.

The present authors have estimated the disalignment rate $\gamma_2-\gamma_0$ of the Ne $2p_2$ level in a cylindrical discharge plasma [23] by the same method as described in Ref. [24] with a modification in the apparatus [25]. A disalignment rate 1.7×10^6 s^{-1} has been obtained for the optical thickness at the line center 0.04, 0.10, 0.01, and 0.04 of the branching transitions to the $1s_2$, $1s_3$, $1s_4$, and $1s_5$ states. Although the geometry assumed in the present simulation is different from the experiment, we may compare the experiment with the simulation result $(3\pm0.5)\times10^6$ s^{-1} (see Ref. [3] for the case where branching transitions are present). If we take into account the difference, the agreement between these results is satisfactory since the plane parallel geometry is more effective in disalignment by, roughly speaking, a factor of 2 under the condition of low optical thickness.

The influence of the alignment relaxation by radiation trapping upon radiative lifetime measurements has been discussed recently [5,7,26]. The present Monte Carlo simulation has clarified the following two points. First, at $t<1/(\gamma_2-\gamma_0)$ the proportional factor of the observed emission line intensity to the upper level population varies with time and therefore the observed decay rate is different from the real decay rate of the population. The error in the apparent lifetime estimated from the emission intensity increases as the optical thickness increases. Second, at $t>1/(\gamma_2-\gamma_0)$ the proportional factor is almost constant so that the apparent or prolonged lifetime by radiation trapping under the given experimental conditions can be correctly determined free from alignment effects. Assuming that atoms are optically excited and that the emission is observed perpendicularly to the quantization axis (the direction of electric vector in case of linearly polarized light excitation), errors in measured lifetimes induced by the alignment relaxation in the former time domain may be given as $\Delta\tau_0/\tau_0 \approx -W_2(\gamma_2-\gamma_0)\tau_0$ $[(\gamma_2-\gamma_0)\tau_0 \ll 1,\ W_2>0]$ [27], where $\tau_0=1/\gamma_0$ and W_2 is the depolarization coefficient [28]. Here the sensitivity of the detection system is assumed to be independent of the polarization directions. Our simulation has shown that the error $\Delta\tau_0/\tau_0$ reaches values as large as -0.8 at $k_0R=13.6$ in the present geometry. In general, the sense and magnitude of the error depends on the angular-momentum pairs of the transition through W_2 and on the experimental conditions, such as the direction and magnitude of the initial alignment and the direction of observation. When the emission is observed along the quantization axis in the present geometry, even an increase, instead of a decrease, in the observed intensity may be seen at an early time. The error $\Delta\tau_0/\tau_0$ is also affected by the relative sensitivity of the detection system for different polarization directions of radiation.

An absorption line profile often provides information on external perturbations to the atomic states involved in the transition. Collisional broadening of resonance levels of rare gases has been subjected to extensive studies in discharge plasmas [29]. In these experiments, atoms in resonance levels are, in effect, produced by radiation trapping. The profiles of absorption lines originating from these levels are observed and the Lorentzian component of the profile is interpreted as due to the resonance broadening besides the natural broadening. As shown in Fig. 5(b), atoms in the resonance level actually have different temperatures depending on the location of the medium when viewed in the direction perpendicular to the plane; the best-fitted Gaussian profile to the velocity distribution in the perpendicular direction to the planes gives the effective temperature, which is 4–5 % lower (higher) at the center (boundary) than the gas temperature (288.15 K) under this simulation condition (i.e., plane parallel geometry, Gaussian broadening with optical thickness of 13.6 at the line center with no frequency redistribution in the frame of atoms). For cylindrical geometry, it may be assumed that the deviation is larger because at the boundary, excitation by the radiation coming radially with the self-reversal profile is more effective in determining the radial temperature than the corresponding excitation for the plane parallel geometry. Furthermore, since the line profiles in Fig. 5(b) are slightly different from a Gaussian shape, the absorption profile deviates from a Voigt profile, which is a convolution of a Lorentzian and a Gaussian, when the absorption line profile is measured in the direction *perpendicular* to the axis of a discharge tube.

IV. CONCLUSION

The Monte Carlo method has been applied to study the population and alignment relaxation by the trapped line radiation in the infinite plane parallel geometry. It has been found that both population and alignment exhibit nonsingle exponential relaxations, which are interpreted as being due to mixing of the population and alignment caused by the anisotropy of the geometry. After a sufficiently long time, the alignment relaxes at the same rate as the population (*self-alignment*). The influence of the self-alignment to the population relaxation rate is found to be negligible within the uncertainty of the simulation ($<1\%$), in contrast to the analytical estimate by Perel' and Rogova [14]. The population relaxation affected by the alignment mixing is instead seen in the beginning of the relaxation when the alignment is large. The population and alignment relaxation rates in the range of the optical thickness at the line center between 10^{-3} and 10^{2} are derived in a time interval when these mixing effects are negligible. A discrepancy between the simulation and the analytical estimate [3,12] has been found. It has also been demonstrated that the velocity distribution of excited atoms in the direction perpendicular to the planes, both at the center and at the boundaries of the geometry, is substantially different from the distribution at the base temperature.

ACKNOWLEDGMENTS

One of the authors (A.H.) is grateful for financial support from the Axel and Margaret Ax:son Johnson foundation for his stay at the Royal Institute of Technology, Stockholm. The calculation was partly performed on a FACOM M-1800 computer at the National Institute for Fusion Science Computer Center, Japan.

[1] S. Chandrasekhar, *Radiative Transfer* (Dover, New York, 1960).
[2] A. Hishikawa, H. Mizuno, M. Tani, and R. Okasaka, J. Phys. B **25**, 3419 (1992).
[3] T. Holstein, Phys. Rev. **72**, 1212 (1947).
[4] T. Holstein, Phys. Rev. **83**, 1159 (1951).
[5] T. Fujimoto, C. Goto, and K. Fukuda, Phys. Scr. **26**, 443 (1982).
[6] N. Bras, J. Ph. Brunet, J. Butaux, J. C. Jeannet, and D. Perrin, J. Phys. B **17**, 65 (1984).
[7] P. Erman and A. Hishikawa, Phys. Scr. **46**, 348 (1992).
[8] E. B. Salomon and W. Happer, Phys. Rev. **144**, 7 (1966).
[9] K. T. Compton, Phys. Rev. **20**, 283 (1922); E. A. Milne, J. London Math. Soc. **1**, 823 (1926).
[10] L. M. Biberman, Zh. Eksp. Teor. Fiz. **17**, 416 (1947); **19**, 584 (1949).
[11] J. P. Barrat, J. Phys. Radium **20**, 541 (1959); **20**, 633 (1959).
[12] M. I. D'Yakonov and V. I. Perel', Zh. Eksp. Teor. Fiz. **47**, 1483 (1964) [Sov. Phys. JETP **20**, 997 (1965)].
[13] K. Blum, *Density Matrix Theory and Applications* (Plenum, New York, 1981).
[14] V. I. Perel' and I. V. Rogova, Zh. Eksp. Teor. Fiz. **65**, 1012 (1973) [Sov. Phys. JETP **38**, 501 (1974)].
[15] Kh. Kallas and M. Chaika, Opt. Spectrosc. **27**, 376 (1969); M. Lombardi and J. C. Pebay-Peyroula, C. R. Acad. Sci. **261**, 1485 (1965); C. G. Carrington and A. Corney, Opt. Commun. **1**, 115 (1969).
[16] L. W. Avery and L. L. House, Astrophys. J. **152**, 493 (1968); L. L. House and L. W. Avery, J. Quant. Spectrosc. Radiat. Transfer **9**, 1579 (1969).
[17] J. P. Delaboundiniere, J. Quant. Spectrosc. Radiat. Transfer **22**, 411 (1979).
[18] D. R. Hamilton, Astrophys. J. **106**, 457 (1947).
[19] G. J. Parker, W. N. G. Hitchon, and J. E. Lawler, J. Phys. B **26**, 4643 (1993).
[20] J. E. Lawler, G. J. Parker, and W. N. G. Hitchon, J. Quant. Spectrosc. Radiat. Transfer **49**, 627 (1993).
[21] V. I. Perel' and V. Rogova, Zh. Eksp. Teor. Fiz. **61**, 1814 (1971) [Sov. Phys. JETP **34**, 965 (1972)].
[22] J. F. Williams, A. G. Mikosza, J. B. Wang, and A. B. Wedding, Phys. Rev. Lett. **69**, 757 (1992).
[23] T. Fujimoto, C. Goto, Y. Uetani, and K. Fukuda, Phys. Scr. **28**, 617 (1983).
[24] T. Fujimoto, C. Goto, Y. Uetani, and K. Fukuda, J. Appl. Phys. **24**, 875 (1985).
[25] Y. Ishitani, H. Ishida, T. Kitagawa, A. Hishikawa, and T. Fujimoto, J. Phys. B **26**, L671 (1993).
[26] P. Erman, O. Gustafsson, and P. Lindblom, Phys. Scr. **37**, 42 (1988); P. Erman and G. Sundström, Phys. Rev. A **43**, 5790 (1991).
[27] A. Hishikawa, doctoral thesis, Kyoto University, 1994 (unpublished).
[28] A. Omont, C. R. Acad. Sci. **260**, 3331 (1965); A. Hirabayashi, Y. Nambu, and T. Fujimoto, Jpn. J. Appl. Phys. **25**, 1563 (1986).
[29] P. E. G. Baird, K. Burnett, R. Damaschini, D. N. Stacey, and R. C. Thompson, J. Phys. B **12**, L143 (1979); A. C. Lindsay, J. L. Nicol, D. N. Stacey, and P. E. G. Baird, *ibid.* **22**, L303 (1989); A. C. Lindsay, J. L. Nicol, and D. N. Stacey, *ibid.* **24**, 4901 (1991).